Appendix :

Appendix Table S1 : Sequences of the other single siRNA

siRNA	Sense sequence	Antisense sequence
UBTD1single1	CAAGCGAGCAGGACGCAAU	GGAGCAAACGGGAUGAGUU
UBTD1single2	GAAGCAGGUUCGAGCCAC	CCACAAGGGCCAACCAGGA
ROCK1	GGUUAGAACAAGAGGUAAA	CAACCAAGAAAGAGAGAA
ROCK2	UGAAAGAAAUGGAGAAGAA	UGAAAGAGCUGGAGAUCAA
LATS1	CACGGCAAGAUAGCAUGGA	CAUACGAGUCAAUCAGUAA
LATS2	AAAGGCGUAUGGCGAGUAG	GCCACGACUUAUUCUGGAA

Appendix Table S2 : Primer table

	Forward	**Reverse**
RPLP0	GCATCAGTACCCAATTCTATCAT	AGGTGTAATCCGTCTCCACAGA
Snail	TCGGAAGCCTAACTACAGCGA	AGATGAGCATTGGCAGCGAG
fibronectin 1	CGGTGGCTGTCAGTCAAAG	AAACCTCGGCTTCCTCCATAA
aSMA	GCGTGGCTATTCCTTCGTTAC	CATAGTGGTGCCCCCTGATAG
Vimentin	TTTCTCTGCCTCTTCCAAACTTTT	CCTGTCCATCTCTAGTTTCAACCG
birc5	AGCATTCGTCCGGTTGCGCT	TCGATGGCACGGCGCACTTT
cyr61	AGCCTCGCATCCTATACAACC	TTCTTTCACAAGGCGGCACTC
ctgf1	CAGCATGGACGTTCGTCTG	AACCACGGTTTGGTCCTTGG
e-cadherin	GGTGACAGAGCCTCTGGATA	GATGACACAGCGTGAGAGAAG
Slug	CGTAGGATCTCTGGTTGTGGT	CGAACTGGACACACATACAGTG

Appendix Figure S1 :

(A) Representative confocal images of E-cadherin and UBTD1 in confluent DU145 cells under resting (Ctrl), after calcium chelator treatment (EGTA) and recovery (Rec) conditions. E-cadherin is used as a control. (B) Representative confocal images of β-catenin and UBTD1 in confluent A549 cells under resting (Ctrl), after calcium chelator treatment (EGTA) and recovery (Rec) conditions. (C) Representative confocal images of β-catenin and UBTD1 in A549 cells after cell scattering induced by HGF treatment (24 h). (D) Representative confocal images of β-catenin and UBTD1 localization depending on the actin cytoskeleton using cytochalasin D (CytoD) treatment in confluent DU145 cells. (E) Representative confocal images of YAP and UBTD1 localization on two matrices of different stiffnesses. DU145 cells were transfected with the indicated siRNA (control, siCTRL; UBTD1: siUBTD1pool) for 24h and were grown on fibronectin/acrylamide-coated glass coverslips (soft) or directly on glass coverslips (stiff). (F) Representative confocal images of β-catenin and UBTD1 localization in two different cell densities of DU145 cells transfected with the indicated siRNA (control, siCTRL; UBTD1: siUBTD1pool). For microscopy imaging panels (A, B, C, D, E, F), nuclei were stained with DAPI (Blue) on the MERGE image.

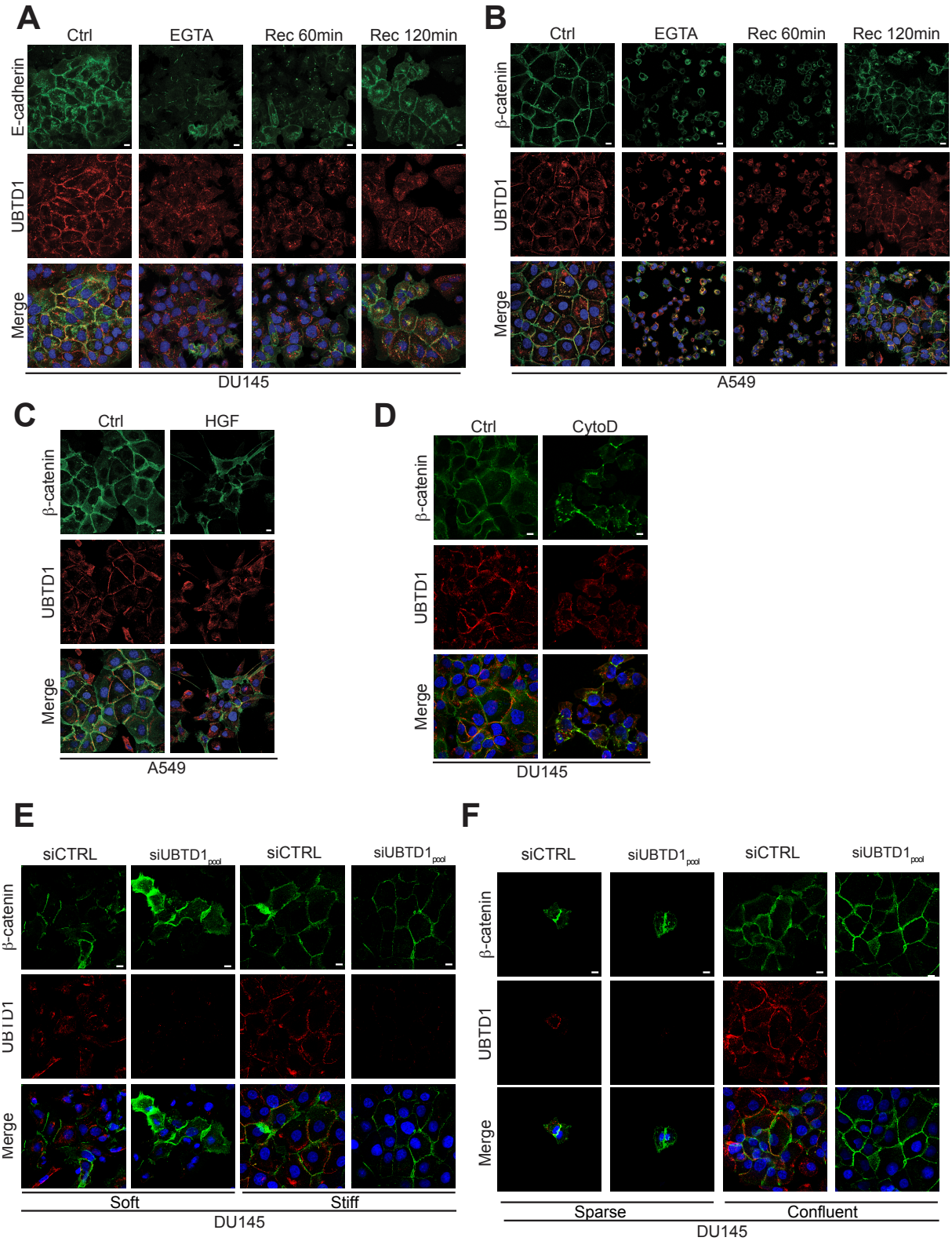

Appendix Figure S1

Appendix Figure S2 :

(A) Immunoblots (up) and quantification (down) of YAP levels in sub-confluent DU145 or A549 UBTD1 depleted cells treated or not with cycloheximide (CHX) for 2h. Immunoblot of UBTD1 shows the level of siRNA depletion. Actin was used as a loading control. (B) Representative wide-field image of proximal ligation assay monitoring (left) and quantification (right) of UBTD1 interaction with YAP depending on actin cytoskeleton using cytochalasin D (CytoD) treatment in DU145 and A549 cells. (C) Representative wide-field image of proximal ligation assay, showing the absence of interaction between UBTD1 and ubiquitin. For microscopy imaging panels (B, C), nuclei were stained with DAPI (Blue) on the MERGE image. (D) The immunoblot of His shows the level of His-Ub transfection for YAP ubiquitylation in HEK cells in Figure 4H.

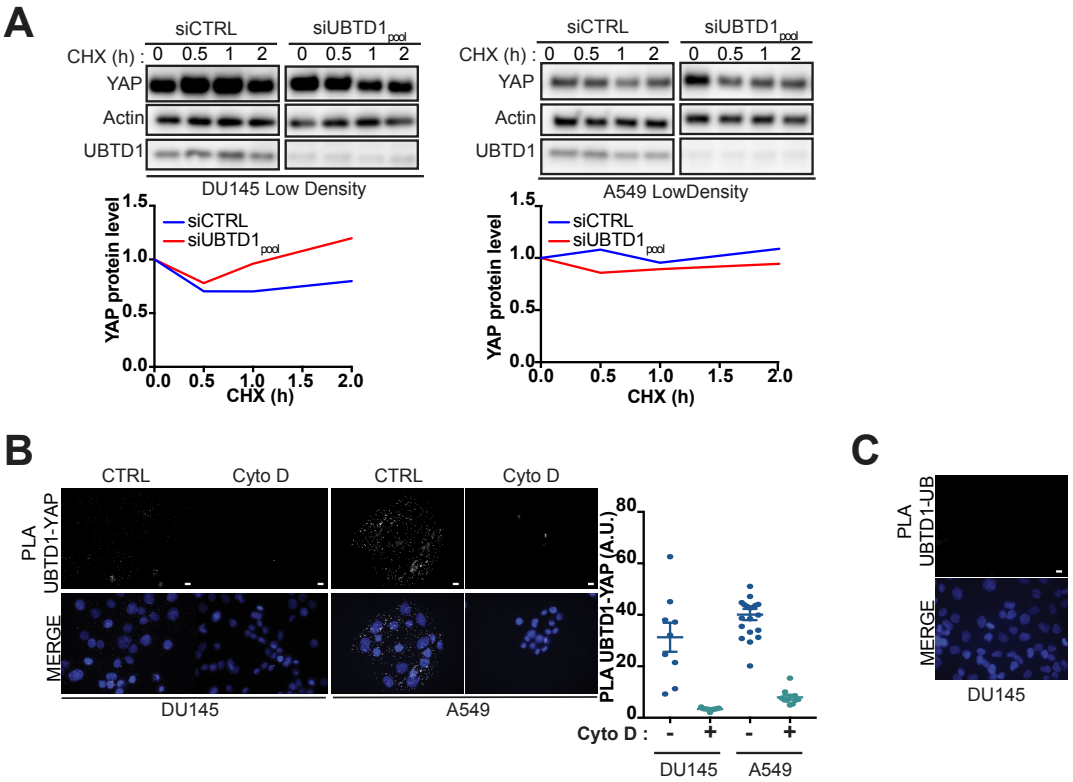

Appendix Figure S2

Appendix Figure S3 :

(A) Immunoblots of p-YAP and YAP in confluent A549 control (siCTRL) or depleted for LATS1 and LATS2 (siLATS1+siLATS2) and/or UBTD1 (siUBTD1pool). Immunoblot of p-YAP reflects the activity of the Hippo pathway. Immunoblots of UBTD1 and LATS show siRNA knock-down efficiency. Actin was used as a loading control. (B-C) Representative confocal immunofluorescence images (B) and quantification (C) showing endogenous YAP nuclear translocation in confluent A459 cells control (siCTRL) or depleted for LATS1 and LATS2 (siLATS1+siLATS2) and/or UBTD1 (siUBTD1pool).

For microscopy imaging panels (B), nuclei were stained with DAPI (Blue) on the MERGE image. Scale bar=10 µm; n≥3 independent experiments; *P<0.05; **P<0.01; ***P<0.001;****P<0.0001; (A) two tailed t-test; (G) Bonferroni's multiple comparison test; data are mean ± s.e.m.

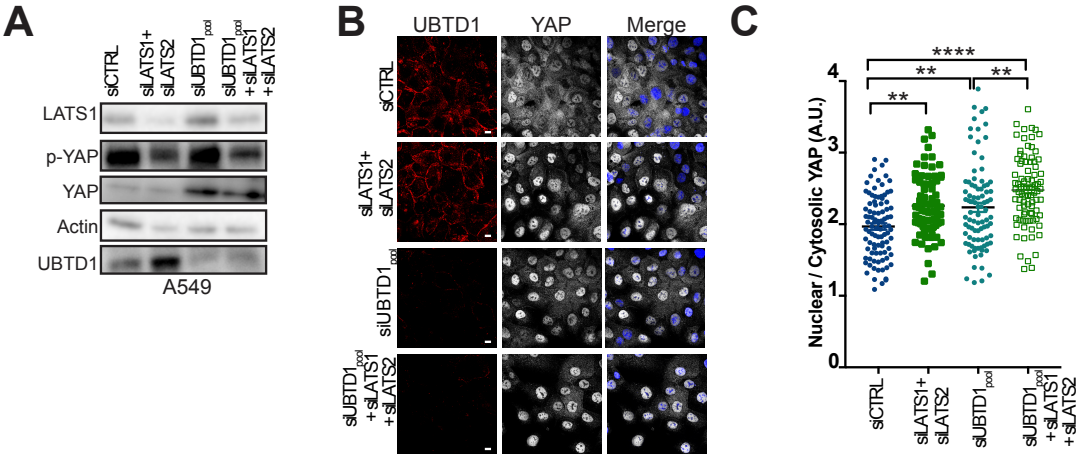

Appendix Figure S3

Appendix Figure S4 :

(A-B) Quantification of CTGF1, CYR61, BIRC5 and UBTD1 mRNA levels in confluent (A) DU145 or (B) A549 cells. (C) Quantification of AMACR and UBTD1 mRNA levels in human prostate tumoroids depleted for UBTD1. AMACR was used as a molecular marker for prostate carcinoma. n≥3 independent experiments; *P<0.05; **P<0.01; ***P<0.001; ****P<0.0001; (A, B) Bonferroni's multiple comparison test; data are mean ± s.e.m.